



# *Contributions to Brain MRI Processing and Analysis*

Dissertation presented to the Department of Computer  
Science and Artificial Intelligence

By

María Teresa García Sebastián

PhD Advisor:

Prof. Manuel Graña Romay



# *Contents*

- ❖ Introduction and Motivation
- ❖ MRI intensity inhomogeneity correction
- ❖ On the detection of Alzheimer's disease
- ❖ Lattice Computing for fMRI analysis
- ❖ Summary of conclusions





# *Contents*

- ❖ Introduction and Motivation
- ❖ MRI intensity inhomogeneity correction
- ❖ On the detection of Alzheimer's disease
- ❖ Lattice Computing for fMRI analysis
- ❖ Summary of conclusions



## *Introduction and motivation*

- ❖ This PhD addresses three issues in the area of medical image processing on MRI:
  - Image preprocessing and segmentation.
  - Image classification.
  - Analysis of functional data.





## *Introduction and motivation*

- ❖ MRI is a very flexible imaging tool:
  - It is a noninvasive imaging procedure.
  - Offers a wide repertoire of pulse sequences for specific visualizations.
  - It can be used for anatomical studies of soft tissues.

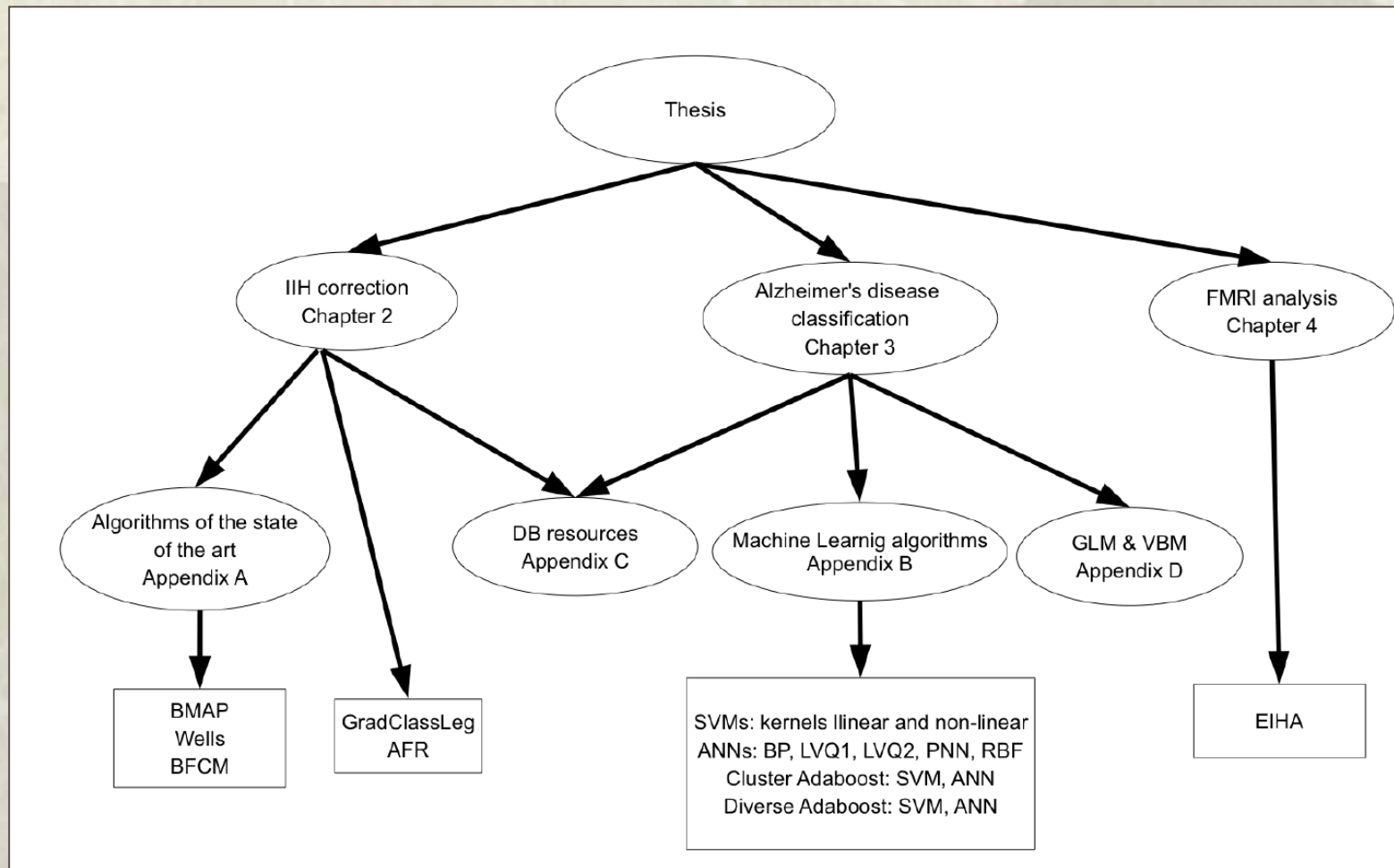


## *Introduction and motivation*

- ❖ This PhD works have been focused on neuroscience applications:
  - Image correction algorithms have been developed and tested on brain volumes.
  - Classification is focused on neurodegenerative diseases.
  - Starting work on functional brain studies.



# Structure of the PhD Thesis





# *Contents*

- ❖ Introduction and Motivation
- ❖ MRI intensity inhomogeneity correction
- ❖ On the detection of Alzheimer's disease
- ❖ Lattice Computing for fMRI analysis
- ❖ Summary of conclusions





# *MRI intensity inhomogeneity (IIH) correction*

- ❖ Introduction
- ❖ Basic assumed image model
- ❖ Our parametric proposal (GradClassLeg)
  - Definition
  - Convergence
  - Results
- ❖ Our non-parametric proposal (AFR, SOM inspired)
  - Definition
  - Convergence
  - Results
- ❖ Conclusions



# *MRI intensity inhomogeneity (IIH) correction*

- ❖ Introduction
- ❖ Basic assumed image model
- ❖ Our parametric proposal (GradClassLeg)
  - Definition
  - Convergence
  - Results
- ❖ Our non-parametric proposal (AFR, SOM inspired)
  - Definition
  - Convergence
  - Results
- ❖ Conclusions





# *Introduction*

- ❖ Theoretically MRI would produce piecewise constant images.
- ❖ Several imaging conditions introduce an additional multiplicative noise factor: the IIH field.
- ❖ IIH is due to the spatial inhomogeneity in the excitatory Radio Frequency signal and other effects.
- ❖ The correction of the IIH artifact is the process of estimating the IIH field and removing this estimation from the given image.



# *Introduction*

There are two kinds of IIH correction algorithms:

- ❖ Parametric: parametric model for the IIH field.
- ❖ Non-parametric: non-parametric estimation of the IIH at each voxel.
  - Most Bayesian image processing approaches.
  - Fuzzy clustering.

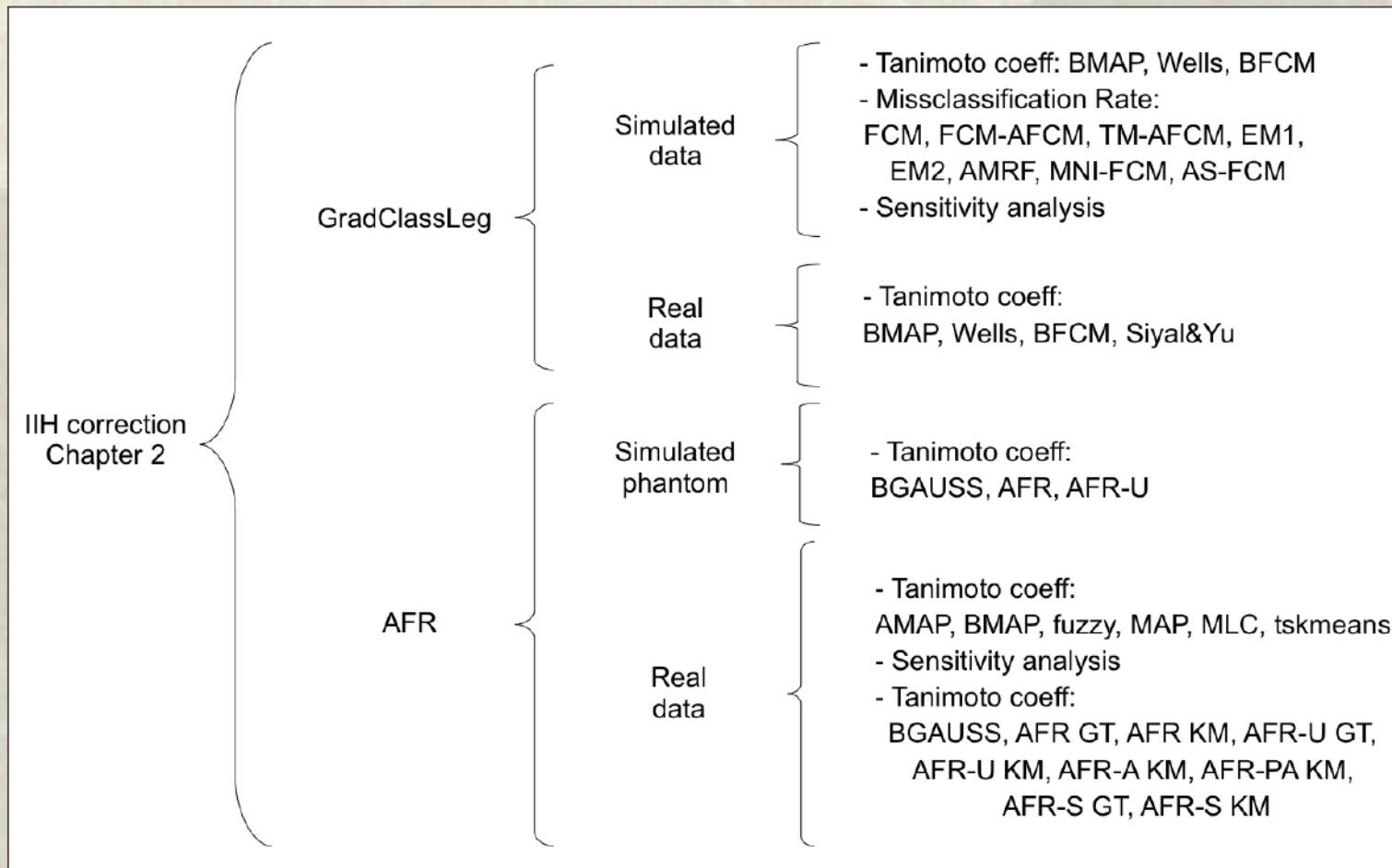
We propose and test two algorithms, one of each kind, for IIH correction.





# Introduction

## summary of the experiments





# *MRI intensity inhomogeneity (IIH) correction*

- ❖ Introduction
- ❖ Basic assumed image model
- ❖ Our parametric proposal (GradClassLeg)
  - Definition
  - Convergence
  - Results
- ❖ Our non-parametric proposal (AFR, SOM inspired)
  - Definition
  - Convergence
  - Results
- ❖ Conclusions





# Image formation model

$$y_i = \beta_i \cdot r_i + \eta_i,$$

Where:

$\mathbf{y} = (y_i; i \in I)$  ;  $i \in I \subset N^3$  is the observed image,

$\beta_i$  is the multiplicative inhomogeneity field,

$r_i$  is the clean signal associated with the true voxel class  $x_i$

$\eta_i$  is the additive noise term



## *Logarithmic model*

- ❖ The image logarithm if we discard the additive noise term

$$Y_i = B_i + R_i,$$

Where:

$$Y_i = \ln y_i, B_i = \ln \beta_i \text{ and } R_i = \ln r_i$$





# *MRI intensity inhomogeneity (IIH) correction*

- ❖ Introduction
- ❖ Basic assumed image model
- ❖ Our parametric proposal (GradClassLeg)
  - Definition
  - Convergence
  - Results
- ❖ Our non-parametric proposal (AFR, SOM inspired)
  - Definition
  - Convergence
  - Results
- ❖ Conclusions



## *GradClassLeg*

- ❖ IIR correction parametric algorithm.
- ❖ Gradient descent of the classification error in images corrected by products of Legendre polynomials.
- ❖ In this approach we work with the original image. We do not perform the logarithm transformation.





# *GradClassLeg*

- ❖ Steps of definition:
  - Definition of the energy function.
  - Energy minimization by gradient descent.
  - Convergence issues.



## Definition

- ❖ IIH 3D field parametric model:

$$\beta_i(\mathbf{p}) = \sum_{j=0}^m \sum_{k=0}^{m-j} \sum_{l=0}^{m-k-j} p_{jkl} P_j(i_x) P_k(i_y) P_l(i_z);$$

- ❖ Energy function:

$$e(\mathbf{p}, \Gamma) = \sum_{i \in I} \left( \frac{y_i}{\hat{\beta}_i(\mathbf{p})} - \mu_{x_i} \right)^2$$





# *Energy minimization*

## ❖ Gradient descent:

- gradient descent on the IH field model parameters.

$$\mathbf{p}_{t+1} = \mathbf{p}_t + \alpha_t^{\mathbf{p}} \nabla_{\mathbf{p}} e(\mathbf{p}, \Gamma),$$

- gradient descent on the class intensity means.

$$\Gamma_{t+1} = \Gamma_t + \alpha_t^{\Gamma} \nabla_{\Gamma} e(\mathbf{p}, \Gamma).$$



## *Energy minimization*

$$\nabla_{\mathbf{p}} e(\mathbf{p}, \Gamma) = \left\{ \frac{\partial}{\partial p_{jkl}} e(\mathbf{p}, \Gamma) \right\}$$

$$\frac{\partial}{\partial p_{jkl}} e(\mathbf{p}, \Gamma) = \sum_{i \in I} \left( \frac{y_i}{\hat{\beta}_i(\mathbf{p})} - \hat{\mu}_{\hat{x}_i} \right) \frac{-y_i P_j(i_x) P_k(i_y) P_l(i_z)}{\hat{\beta}_i^2(\mathbf{p})}$$





# Convexity

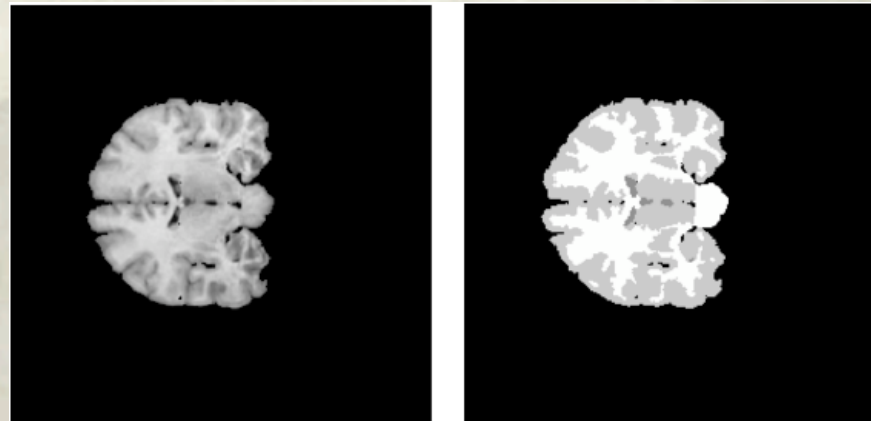
❖ Convexity of the energy function:

$$\frac{\partial^2 e(\mathbf{p}, \Gamma)}{\partial^2 p_{jkl}} = \sum_{i \in I} \frac{\hat{\mu}_{\hat{x}_i} y_i (P_j(i_x) P_k(i_y) P_l(i_z))^2}{\hat{\beta}_i^3(\mathbf{p})}$$
$$\frac{\partial^2 e(\mathbf{p}, \Gamma)}{\partial p_{jkl} \partial p_{mno}} = \sum_{i \in I} \frac{\hat{\mu}_{\hat{x}_i} y_i P_j(i_x) P_k(i_y) P_l(i_z) P_m(i_x) P_n(i_y) P_o(i_z)}{\hat{\beta}_i^3(\mathbf{p})}$$



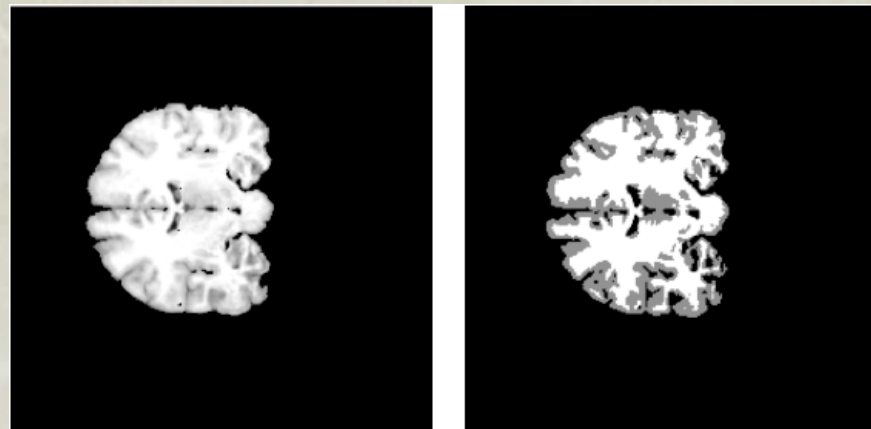
# *Some visual results*

Original



Manual segmentation

IIH  
Corrected



Algorithm's classification





## *Robustness experiments*

- ❖ Experimental data: BrainWeb volumes.
- ❖ Experimental setting:
  - Random initial values of the intensity class means.
  - Application of both gradient rules.
  - Varying interleaving frequency.



# *Robustness computational results*

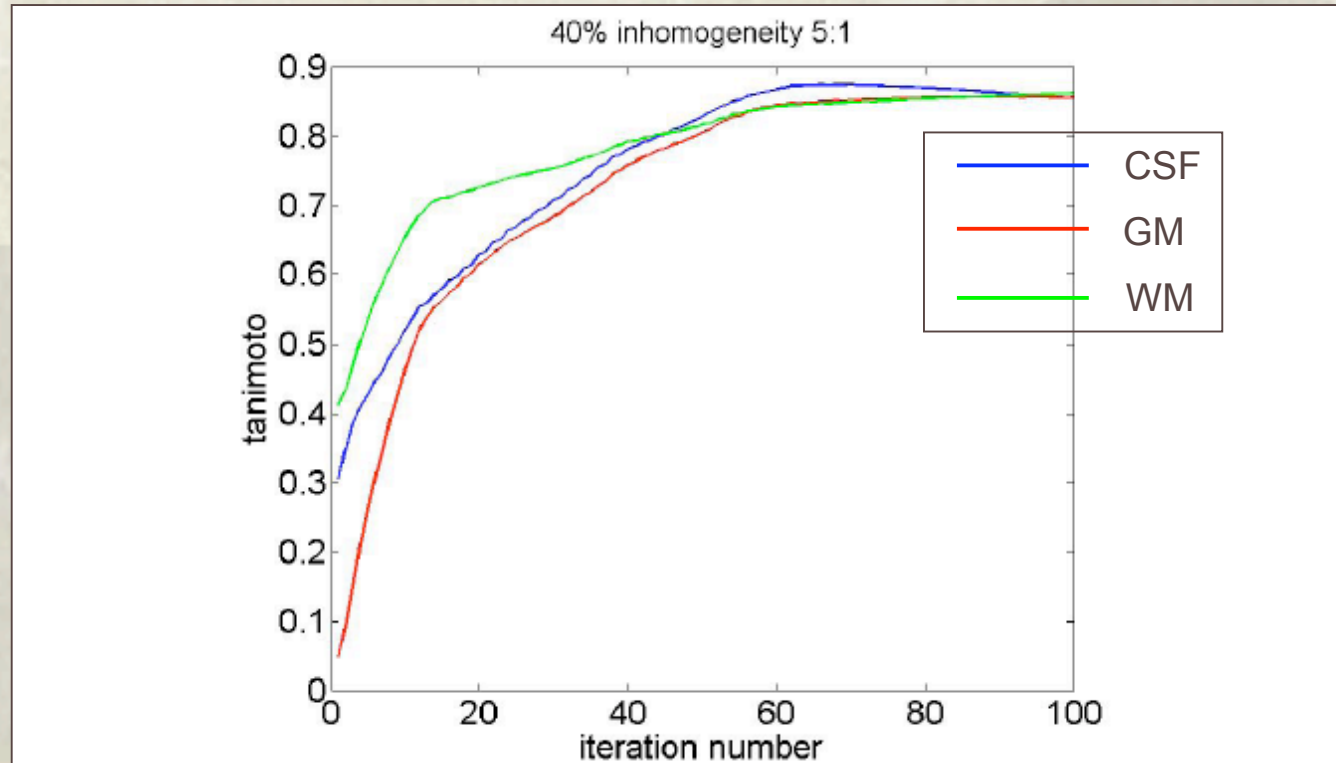


Figure 2.13: Average Tanimoto coefficients for CSF, GM and WM obtained over a simulated 40% IHH inhomogeneity brain volume. Gradient computation relative frequency 5:1 (see text).





## *Some comparative results*

- ❖ Experimental data: IBSR volumes.
- ❖ Experimental settings:
  - Initial intensity class means given by the tissue averages over the manual segmentation.
  - Comparative results obtained from the literature.



## *Comparative results*

Algorithm	GM	WM
Wells	0.564	0.567
BMAP	0.558	0.562
BFCM	0.630	0.709
Modified FCM [148]	0.750	0.724
GradClassLeg	0.745	0.732

Table 2.2: The average Tanimoto coefficients for GM and WM classes over the IBSR collection between manual segmentation and the segmentation results of GradClassLeg, BMAP, BFCM and Modified FCM for the real data.





# *MRI intensity inhomogeneity (IIH) correction*

- ❖ Introduction
- ❖ Basic assumed image model
- ❖ Our parametric proposal (GradClassLeg)
  - Definition
  - Convergence
  - Results
- ❖ Our non-parametric proposal (AFR, SOM inspired)
  - Definition
  - Convergence
  - Results
- ❖ Conclusions



## *Adaptive field rule (AFR)*

- ❖ IIR correction non-parametric algorithm.
- ❖ Gradient descent of an energy function that involves the smoothing of the errors in the neighbourhood of the voxel.
- ❖ For this approach we perform the logarithm transformation of the original image.





# *Energy formulation*

Spatial independent energy function:

$$E(\mathbf{y}; \Gamma, \beta) = \sum_i \left( \frac{y_i}{\beta_i} - \mu_{c(i)} \right)^2,$$

Where:

$$\Omega = \{\omega_1, \dots, \omega_c\}$$

is the set of the tissue classes.

$$\Gamma = \{\mu_{\omega_1}, \dots, \mu_{\omega_c}\}$$

is the set of the signal intensity values.

$$c(i) = \arg \min_k \left\{ \left\| \mu_k - \frac{y_i}{\beta_i} \right\| \right\}$$



## *Logarithmic transformation*

- ❖ To estimate the inhomogeneity field, we perform the minimization of the energy function:

$$\beta^* = \arg \min_{\beta} E(\mathbf{y}; \Gamma, \beta).$$

- ❖ For simplicity, the energy function is formulated over the logarithmic transformation:

$$\mathbf{B}^* = \arg \min_{\mathbf{B}} \sum_i (Y_i - B_i - M_{c(i)})^2 = \arg \min_{\mathbf{B}} E(\mathbf{Y}; \mathbf{B}, \mathbf{M})$$

Where:

$$Y_i = \log y_i, B_i = \log \beta_i \text{ and } M_{c(i)} = \log \mu_{c(i)}$$





## *Smoothness constraint*

- ❖ The IIH field is usually assumed to be smooth.
- ❖ The energy function does not embody any smoothness constraint.

To regularise the energy function we introduce a smoothness constraint in the model:

$$\forall i, j, k; |i - j| < |i - k| \Rightarrow \|\beta_i - \beta_j\| < \|\beta_i - \beta_k\|$$



## *Energy function*

- ❖ The energy function embodies some smoothness constraints.

$$E_{\sigma}(\mathbf{Y}; \mathbf{B}, \mathbf{M}) = \sum_i \sum_j h_{\sigma}(i - j) (Y_j - B_j - M_{c(j)})^2$$

- ❖ The smoothness constraints implies a topology preservation constraint.





## *Estimation rule*

- ❖ The minimization by gradient descent gives us the estimation rule.

$$\Delta B_i = -2\alpha \sum_j h_\sigma(i - j) (Y_j - B_j - M_{c(j)})$$

- ❖ The smoothness of the resulting IIR field estimation is proven in the Thesis.

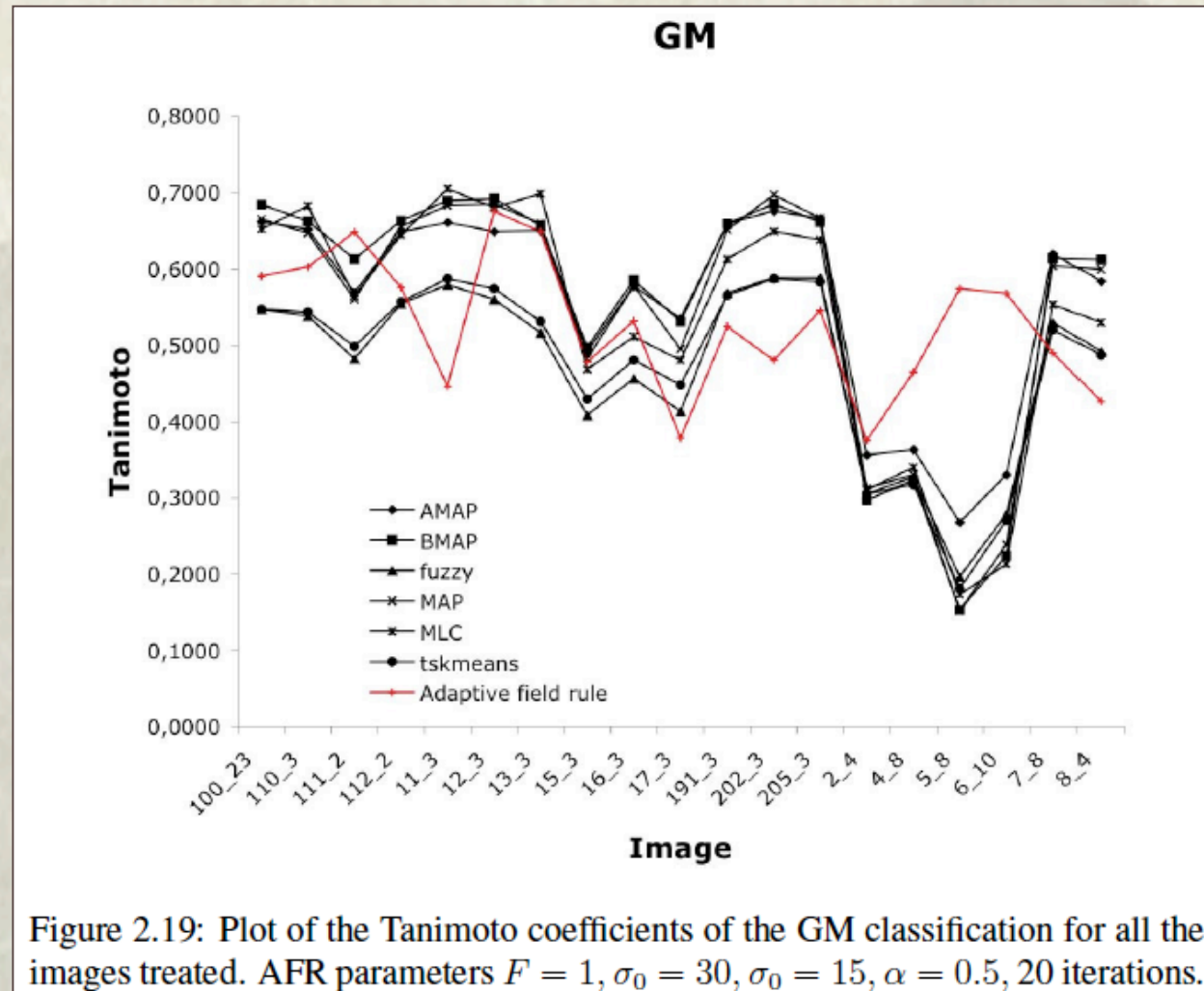


## *Some comparative results*

- ❖ Experimental data: IBSR.
- ❖ The intensity class means are given from the *a priori* knowledge of the manual segmentation.
- ❖ Nominal settings of the parameters.



# Comparative results





## Comparative results

Methods	CSF	GM	WM
Adaptive MAP[127]	0,0697	0,5588	0,5611
Biased MAP[127]	0.0714	0.5527	0.5559
Fuzzy c-means [18]	0.0484	0.4698	0.5608
Maximum A Posteriori Probability (MAP)	0.0714	0.5452	0.5473
Maximum-Likelihood (MLC)	0.0631	0.5317	0.5444
Tree-structure k-means	0.0499	0.4742	0.5653
Adaptive Field Rule (AFR)	0.0918	0.5570	0.5867

Table 2.3: Summary Tanimoto coefficient results for the AFR compared with results, from the IBSR site, of various algorithms.



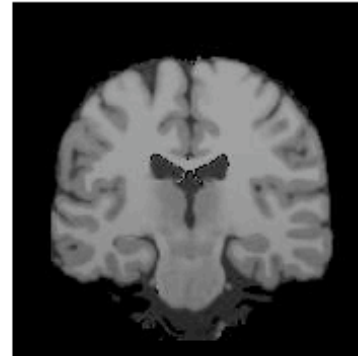


## *Supervised vs. unsupervised*

- ❖ Experimental data: BrainWeb volumes.
- ❖ Compare supervised and unsupervised approaches:
  - BGAUSS: basic supervised Gaussian classifier.
  - AFR: with the intensity class means estimated from the manual segmentation.
  - AFR-U: fully unsupervised, includes intensity class means estimation.

## *Some visual results*

Original



(a)

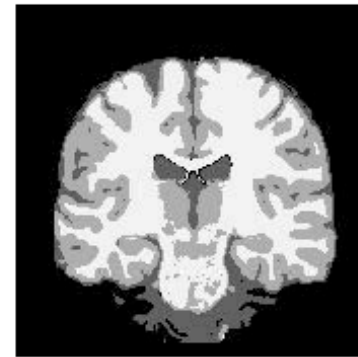


(b)

AFR



(c)



(d)

Ground truth

AFR-U

Figure 2.25: Classification results for one coronal slice of the simulated brain phantom volume with 40% Intensity Inhomogeneity from the BrainWeb site. (a) original skull stripped slice, (b) tissue distribution in the anatomic model providing the classification ground truth, (c) classification after IIIH estimation and correction with AFR, (d) classification after IIIH and intensity class means estimation with AFR-U.





## Comparative results

%IIH, %noise	BGAUSS	AFR	AFR-U
20, 0	(0.95, 0.88, 0.92)	(0.94, 0.89, 0.92)	(0.94, 0.90, 0.94)
20, 3	(0.94, 0.85, 0.90)	(0.93, 0.84, 0.92)	(0.93, 0.89, 0.93)
20, 5	(0.86, 0.80, 0.86)	(0.87, 0.82, 0.88)	(0.88, 0.86, 0.90)
20, 7	(0.81, 0.73, 0.81)	(0.82, 0.79, 0.85)	(0.83, 0.80, 0.86)
→ 20, 9	(0.76, 0.66, 0.77)	(0.78, 0.70, 0.79)	(0.80, 0.76, 0.80)
40, 0	(0.91, 0.79, 0.85)	(0.89, 0.83, 0.90)	(0.89, 0.85, 0.92)
40, 3	(0.90, 0.78, 0.84)	(0.89, 0.81, 0.89)	(0.88, 0.83, 0.91)
40, 5	(0.84, 0.74, 0.82)	(0.88, 0.77, 0.86)	(0.86, 0.77, 0.87)
40, 7	(0.78, 0.65, 0.79)	(0.82, 0.67, 0.81)	(0.82, 0.67, 0.81)
40, 9	(0.73, 0.55, 0.75)	(0.75, 0.59, 0.75)	(0.76, 0.59, 0.75)

Table 2.5: Tanimoto coefficients for CSF, GM and WM tissue classes obtained on the BrainWeb. The simulated phantom has been corrupted with additive noise and IIH.



# *MRI intensity inhomogeneity (IIH) correction*

- ❖ Introduction
- ❖ Basic assumed image model
- ❖ Our parametric proposal (GradClassLeg)
  - Definition
  - Convergence
  - Results
- ❖ Our non-parametric proposal (AFR, SOM inspired)
  - Definition
  - Convergence
  - Results
- ❖ Conclusions





## *IIH correction conclusions*

- ❖ GradClassLeg parametric modeling approach makes it better suited for problems with global smooth variations of the IIH.
- ❖ AFR's non-parametric nature makes it better suited for the detection of local IIH features in MRI data, such as partial volume effects.



## *GradClassLeg conclusions*

- ❖ GradClassLeg assumes that the IIH field model is a linear combination of outer products of 1D Legendre polynomials:
  - IIH model parameters.
  - the intensity class means.
- ❖ We have shown that it can be very robust against bad initial estimations of the intensity class means.
- ❖ Gives comparable results to state of the art algorithms.
- ❖ The classification component of this algorithm is rather naive. It can be expected that the results could improve if the proposed parametric IIH field estimation is combined with more sophisticated classification schemes.





## *AFR conclusions*

- ❖ Adaptive Field Rule (AFR) is the gradient descent of an energy function that involves the smoothing of the errors in the neighborhood of the voxel.
- ❖ It is based on a topological preservation formulation of the smoothness constraint on the IIH field.
- ❖ The results show that AFR gives state of the art results, under the assumption of the knowledge of the intensity class means.



# *Contents*

- ❖ Introduction and Motivation
- ❖ MRI intensity inhomogeneity correction
- ❖ On the detection of Alzheimer's disease
- ❖ Lattice Computing for fMRI analysis
- ❖ Summary of conclusions





# *On the detection of Alzheimer's disease*

- ❖ Introduction
- ❖ Classification process
- ❖ Some results
- ❖ Conclusions and further work



# *Introduction*

- ❖ Alzheimer's Disease (AD):
  - Neurodegenerative disorder and one of the most common cause of dementia in old people.
  - Incurable, degenerative and terminal.
  - Definitive diagnosis can only be made after a post-mortem study of the brain tissue.
  - sMRI scans of the brain may detect changes on the AD patient's brain decades before the first clinical signs of dementia occur.





# *Introduction*

- ❖ **Voxel-Based Morphometry (VBM):**
  - Morphometry analyses allow a comprehensive measurement of structural differences within or across groups.
  - VBM measures differences in local concentrations of brain tissue, through a voxel-wise comparison of multiple brain images.



# *Introduction*

## ❖ Objective:

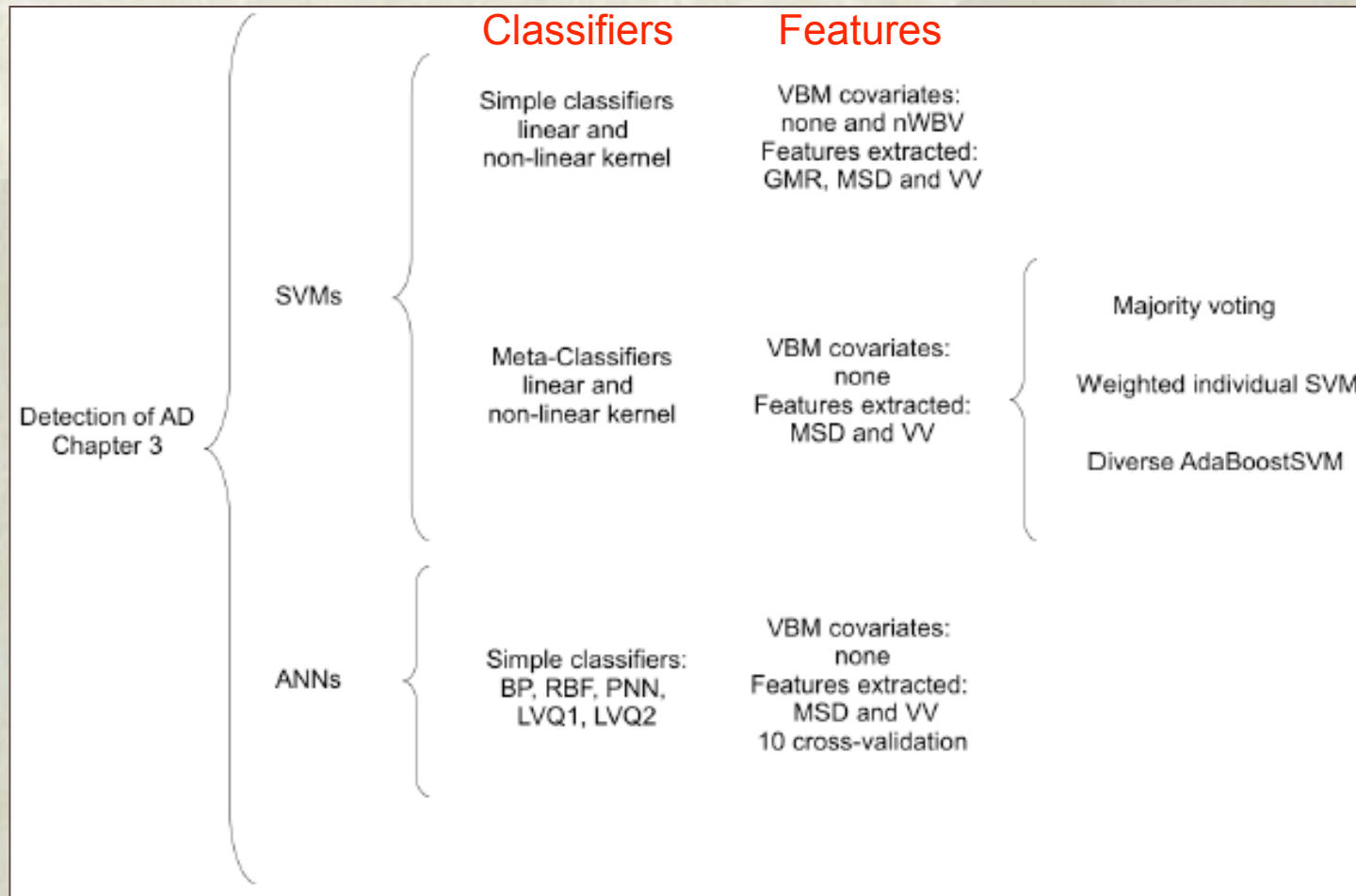
- Early detection of AD patients.
- Using sMRI and Machine Learning tools:
  - Feature extraction based on VBM analyses.
  - Classification using Support Vector Machine (SVM) and Artificial Neural Networks (ANNs).



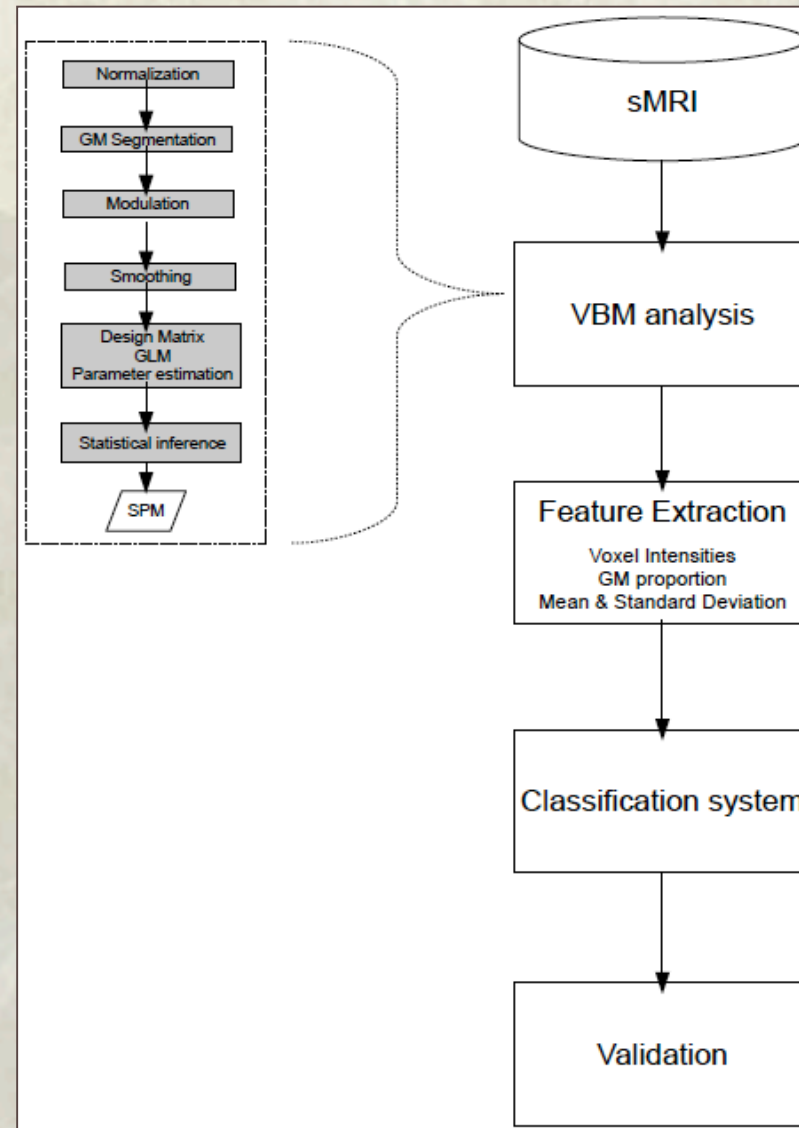


# Introduction

## Summary of the experiments



# Classification process







## *Experimental validation*

- ❖ Experimental data: OASIS database.
- ❖ Some visual results of the VBM analysis.
- ❖ The best classification results (10 fold cross-validation).
  - Single classifiers:
    - SVM.
    - ANN.
  - Meta-classifiers.

## *Segmentation results*

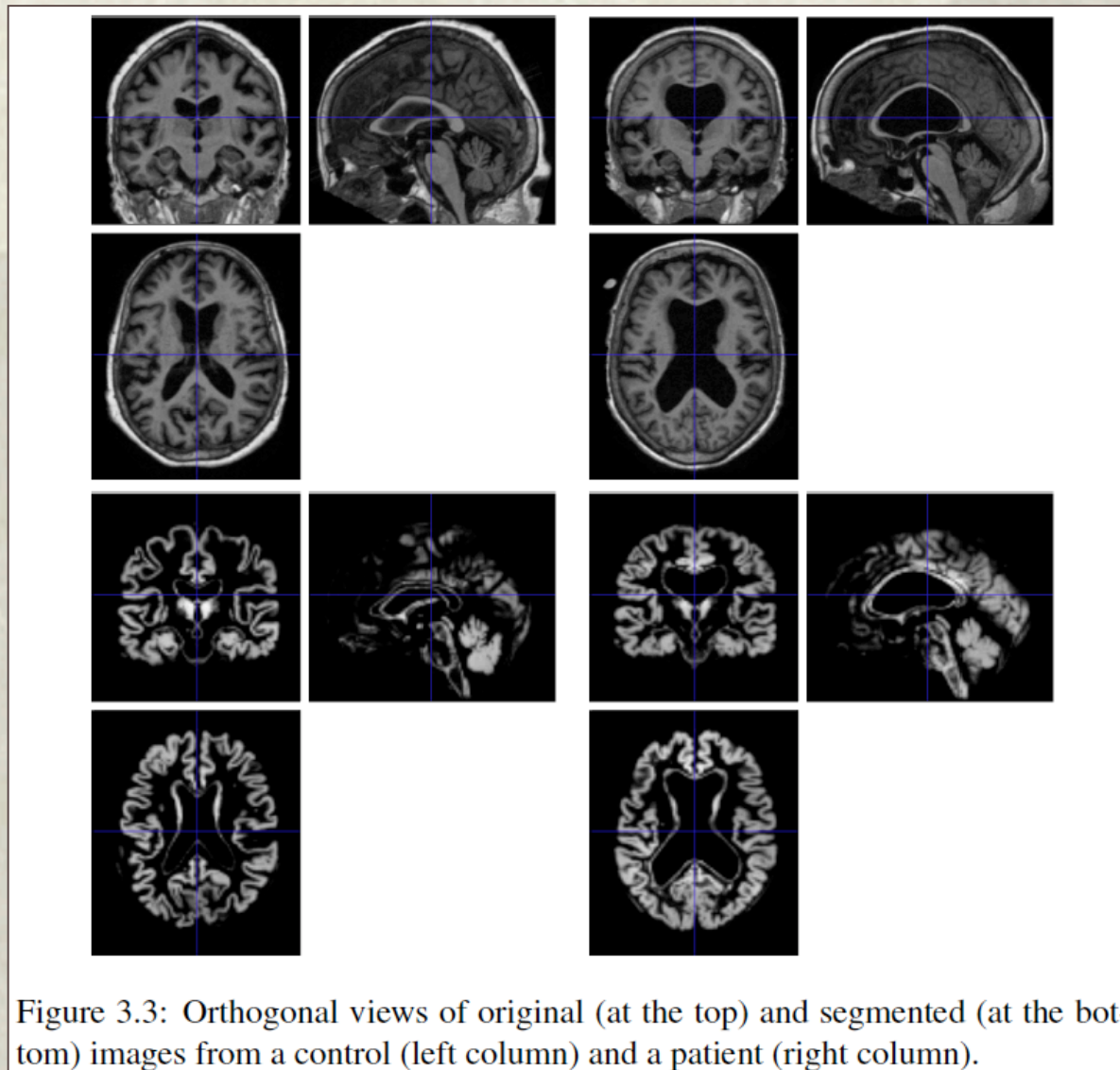
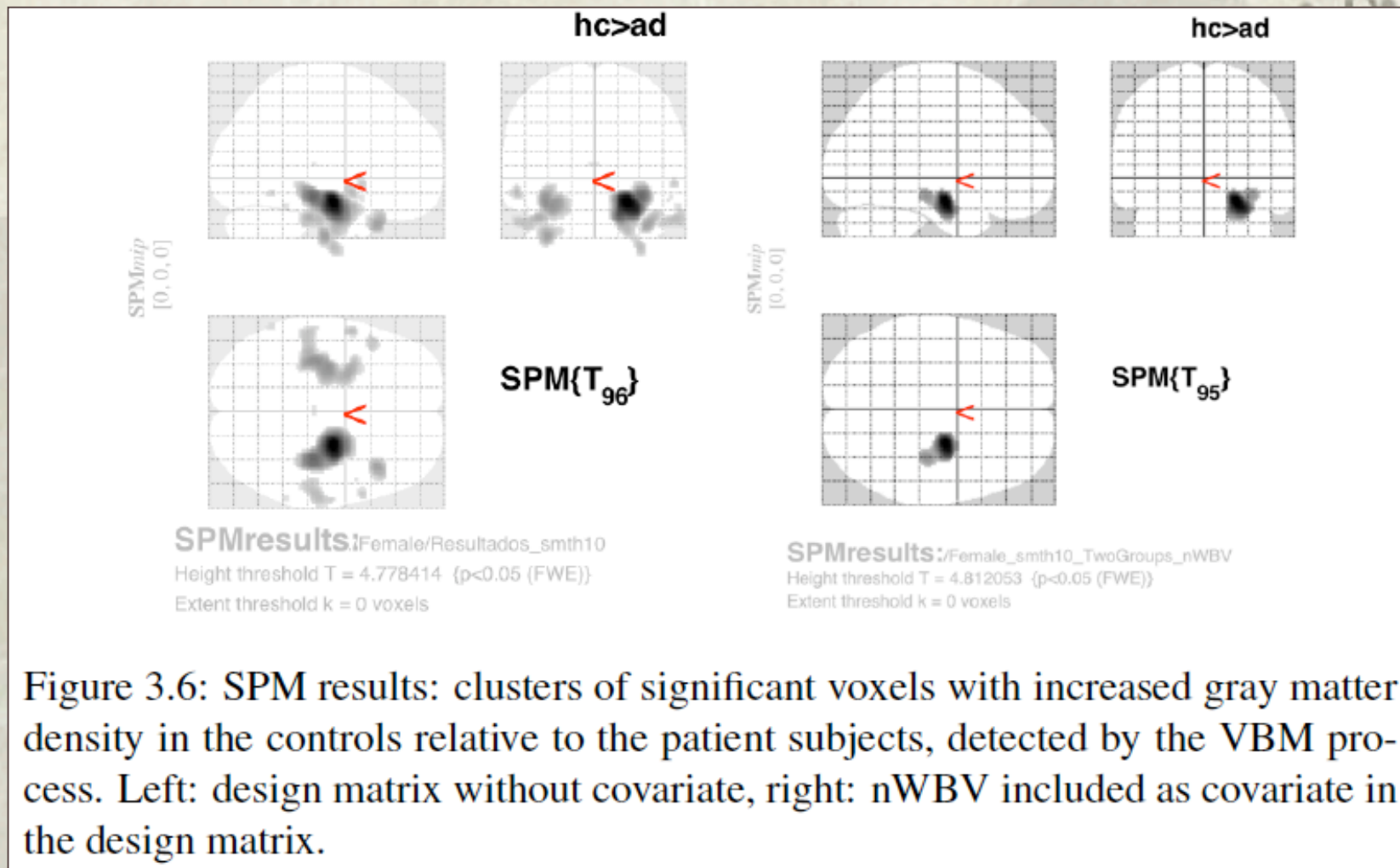


Figure 3.3: Orthogonal views of original (at the top) and segmented (at the bottom) images from a control (left column) and a patient (right column).



# Results after VBM analysis





## *Some classification results*

### ❖ Single SVM classifiers:

Feature extracted	Features	Accuracy (lk/nlk)	Sensitivity (lk/nlk)	Specificity (lk/nlk)
GMR	12	69.39% / 68.36%	0.63 / 0.61	0.88 / 0.90
MSD	24	78.57% / 80.61%	0.72 / 0.75	0.88 / 0.89
VV	3611	73.47% / 76.53%	0.72 / 0.77	0.75 / 0.76

Table 3.4: Classification results with a linear kernel (lk) and a nonlinear kernel (nlk). No covariates have been taken into account in the GLM used for the VBM. The values of  $\gamma = (2\sigma^2)^{-1}$  for non linear kernel were 0.5, 0.031, 0.0078 for each feature extraction process, respectively.





## *Some classification results*

### ❖ Single ANN classifiers:

Feature extracted	Features	Hidden units	Accuracy	Sensitivity	Specificity
MSD	24	10	83%	0.74	0.92
VV	3611	10	77%	0.76	0.78

Table 3.14: Classification results with a LVQ2 network. Network training parameters: MSD: 200 epochs, goal: 0.01 and learning rate: 0.01; VV: 50 epochs, goal: 0.01 and learning rate: 0.005.



## *Some classification results*

### ❖ Meta-classifiers:

Feature extracted	Features	Accuracy (lk/nlk)	Sensitivity (lk/nlk)	Specificity (lk/nlk)
MSD	24	71% / 79%	0.54 / 0.78	0.88 / 0.80
VV	3611	73% / 86%	0.76 / 0.80	0.70 / 0.92

Table 3.8: Weighted individual SVM per cluster classification results. The value of the RBF kernels for the nonlinear (nlk) classifiers were searched for the best fit to the training set.





## *Conclusions and further work*

- ❖ We have studied feature extraction processes based on VBM analysis, to classify MRI volumes of AD patients and normal subjects.
- ❖ The basic GLM design without covariates can detect subtle changes between AD patients and controls that lead to the construction of single (SVMs and ANNs) and meta-classifiers (cluster AdaBoost and diverse Adaboost).



# *Conclusions and further work*

## Summary of best results

		Accuracy	Sensitivity	Specificity	Feature extracted
Single classifiers (table 3.14)	LVQ2	83%	0.74	0.92	MSD
Meta-classifiers (table 3.8)	Weighted individual SVM	86%	0.80	0.92	VV

The weighted cluster SVM and the Diverse AdaBoost SVM methods improved remarkably the results, mainly the sensitivity of the classification models.





## *Conclusions and further work*

- ❖ Further work may address the extraction of features based on other morphological measurement techniques:
  - Deformation-Based Morphometry (DBM).
  - Tensor-Based Morphometry (TBM).



# *Contents*

- ❖ Introduction and Motivation
- ❖ MRI intensity inhomogeneity correction
- ❖ On the detection of Alzheimer's disease
- ❖ Lattice Computing for fMRI analysis
- ❖ Summary of conclusions





# *Lattice Computing for fMRI analysis*

- ❖ Introduction and motivation
- ❖ Description of the approach
- ❖ The linear mixing model
- ❖ Results on a case study
- ❖ Conclusions and further work



# *Introduction*

- ❖ Motivation: explore the applicability of Lattice Computing to perform a kind of non-linear Independent Component Analysis (ICA).





# *Introduction*

- ❖ Current techniques for fMRI analysis:
  - SPM: statistical parametric maps.
    - General Linear Model.
    - Statistical inference (t-test, F-test).
    - Random Field Theory to set the test threshold.
  - ICA: linear source deconvolution.
    - Statistically independent sources.
    - Mixing Matrix.



## *Introduction*

- ❖ SPM is a kind of supervised approach.
  - Experimental settings are included in the GLM design matrix.
  - Suited for block design experiments.
  - Not suited for event driven experiments.
  - The aim is to discover voxel sites that show correlations of BOLD signal and the experimental design.





# *Introduction*

- ❖ Lattice Independent Component Analysis:
  - A mixture of a linear and non-linear approach.
    - Linear Mixing Model.
    - Lattice Autoassociative Memories.
  - Endmembers are equivalent to ICA's independent sources and the GLM's design matrix.



# *Introduction*

- ❖ Lattice Independent Component Analysis can be suited:
  - to discover patterns in the voxel's activations.
  - for event driven experiments.
  - for the study of brain connectivity.





## *General description*

### **Algorithm 4.1** Lattice Independent Component Analysis

Given a fMRI data organized as a set of time series  $X \in \mathbb{R}^{N \times T}$ , where  $N$  is the number of voxels and  $T$  the time duration

1. Apply EIHA to obtain endmembers  $E = \mathbb{R}^{c \times T}$
2. For each voxel compute the endmember abundance coefficients by ULSE, obtaining  $A = \mathbb{R}^{N \times c}$ .
3. For each abundance volume  $A(:, k) = \mathbb{R}^N$  detect the statistical significant voxels as follows:
  - (a) Compute the empirical distribution of the abundance values
  - (b) Set the significance threshold to the 99% percentil value.



## *Linear Mixing Model*

$$\mathbf{x} = \sum_{i=1}^M a_i \mathbf{s}_i + \mathbf{w} = \mathbf{S}\mathbf{a} + \mathbf{w},$$

**a** The abundance vector.

**w** The additive observation noise vector.

Linear unmixing by Unconstrained Least Squares estimation:

$$\hat{\mathbf{a}} = (\mathbf{S}^T \mathbf{S})^{-1} \mathbf{S}^T \mathbf{x}.$$





## *Results on a case study*

- ❖ Auditory stimulation test data of a single person.
- ❖ Data noise has been removed by adequate preprocessing.
- ❖ Successive blocks alternated between rest and auditory stimulation, starting with rest.
  - Auditory stimulation was bi-syllabic words presented binaurally at a rate of 60 per minute.



## *Results on a case study*

- ❖ We have computed:
  - An standard SPM study.
  - Our Lattice Independent Component Analysis.
    - Activation is detected by 99% percentile thresholding for both.
- ❖ Aim:
  - Test that our approach behaves comparably to established approaches in well known datasets.





## *Results on a case study*

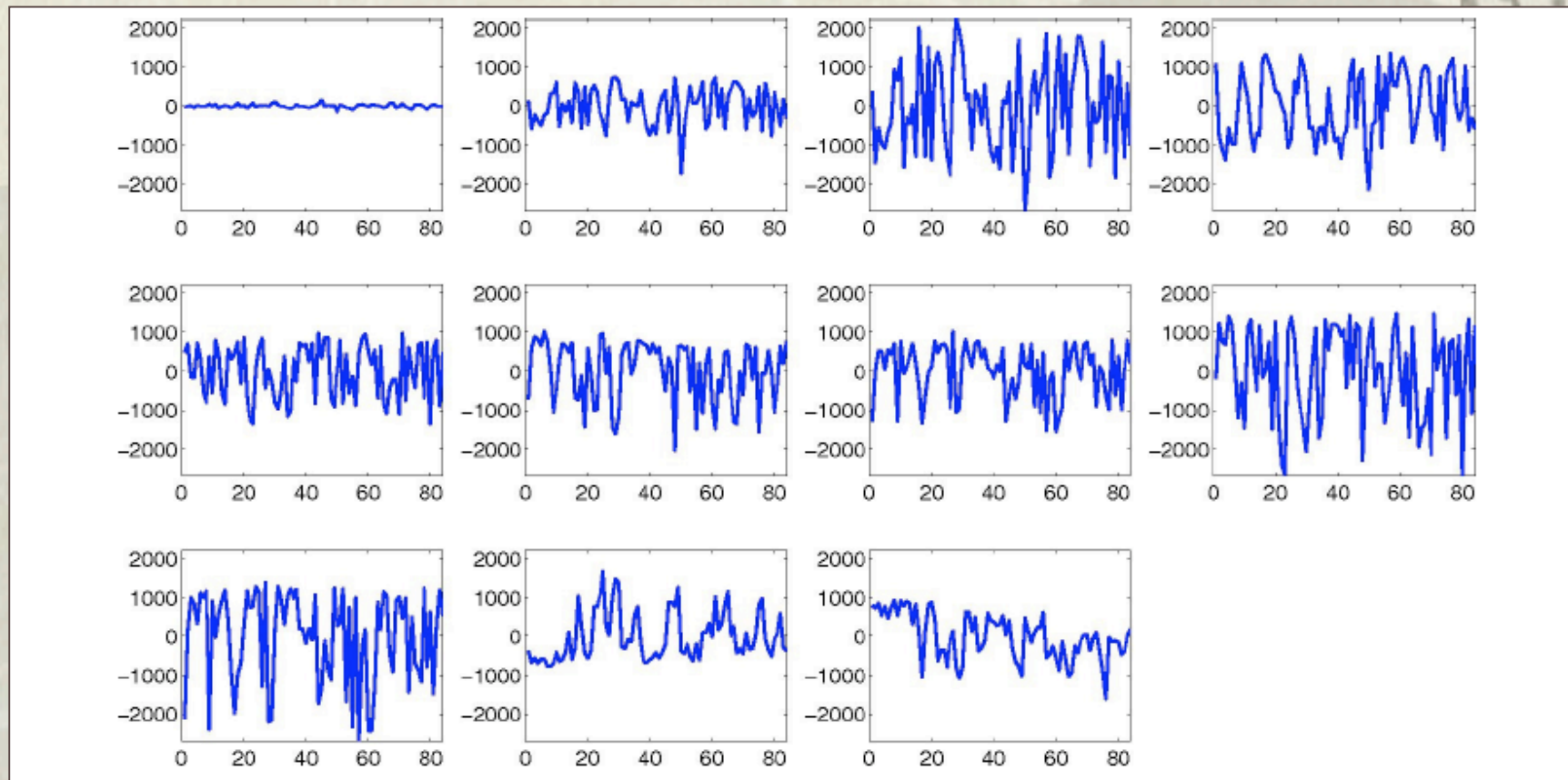


Figure 4.3: Eleven endmembers detected by EIHA over the lattice normalized time series of the whole 3D volume.

# *Results on a case study*

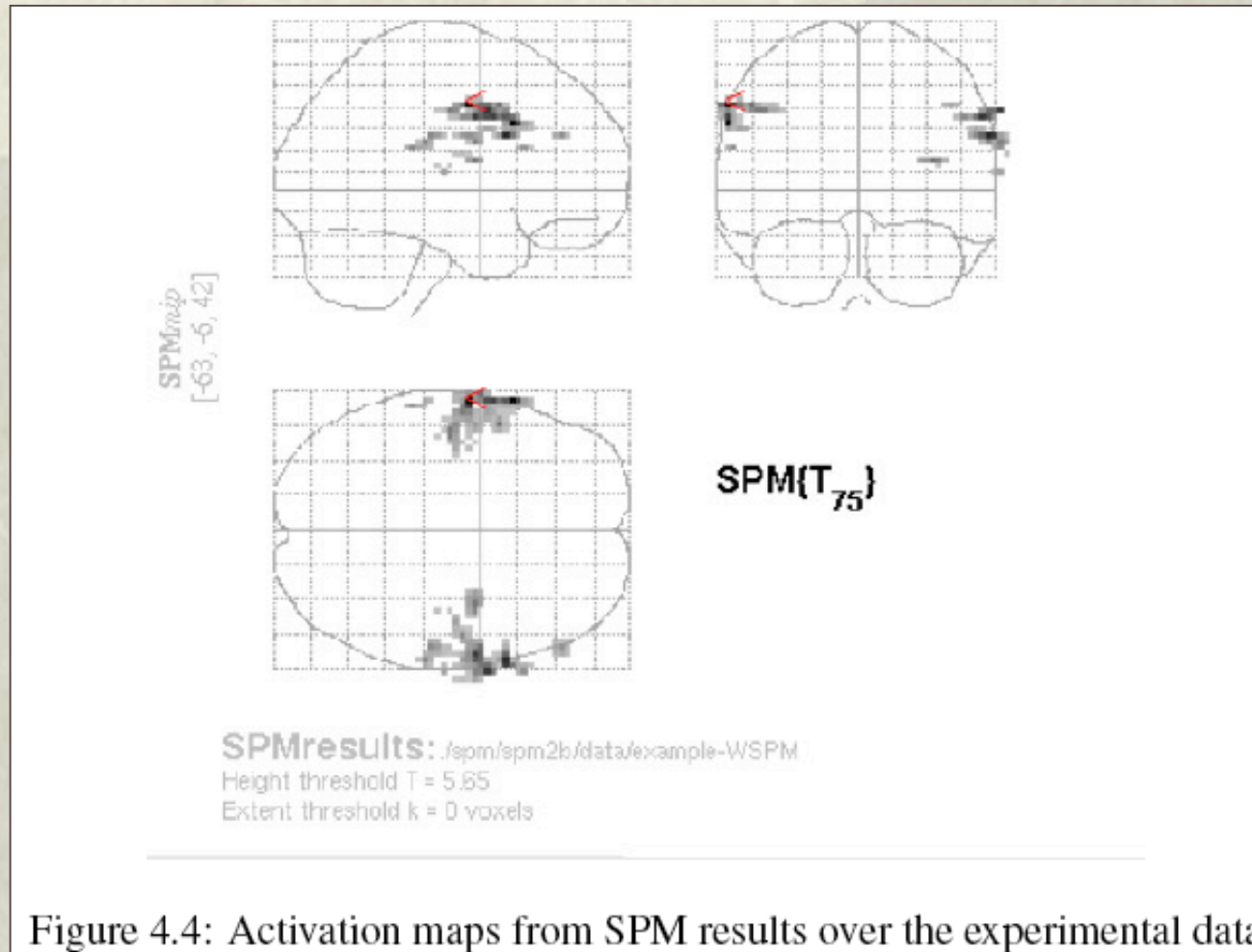


Figure 4.4: Activation maps from SPM results over the experimental data



## *Results on a case study*

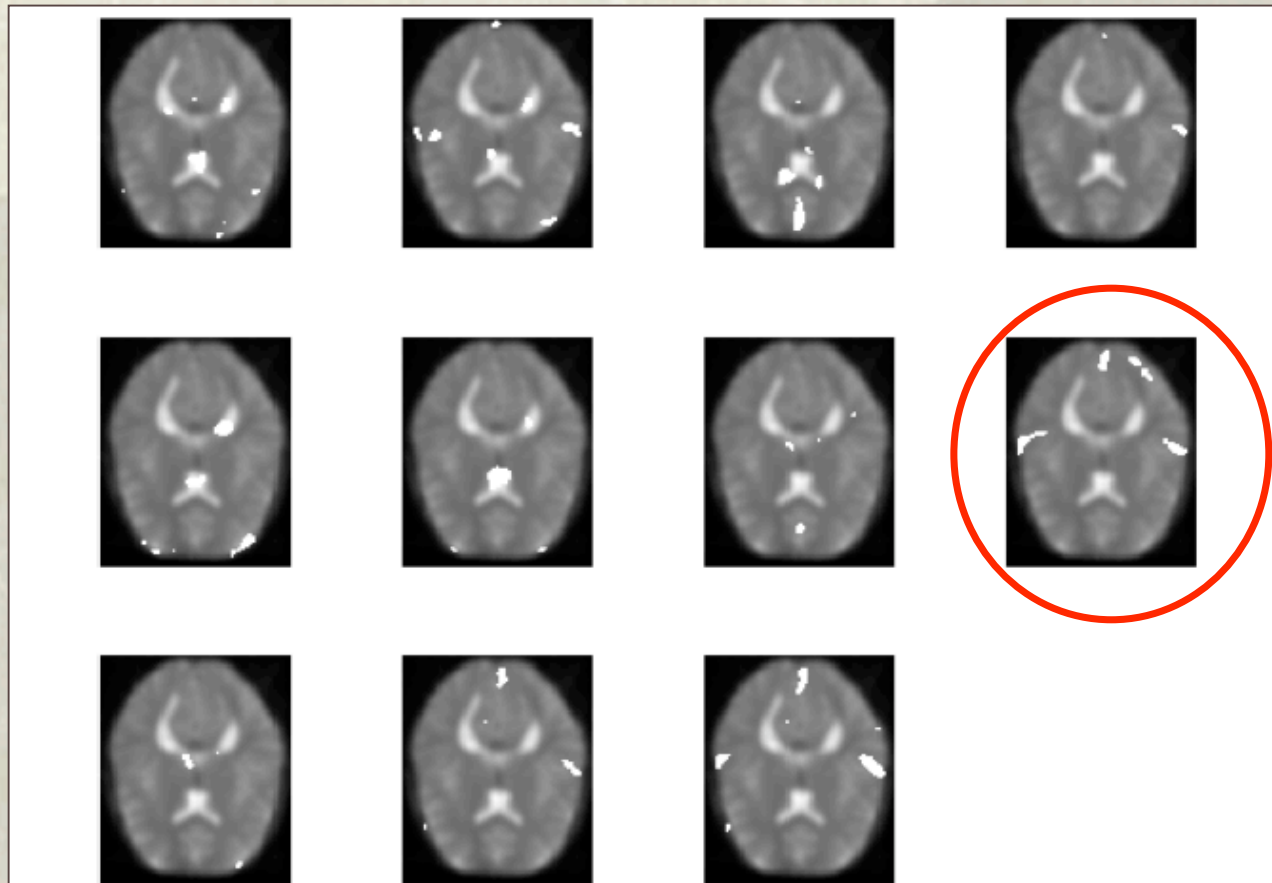


Figure 4.5: Abundances for axial slice #30 for all eleven endmembers. White voxels correspond to abundance values above the 99% percentile of the distribution of the abundances for each endmember at this slice.



## *Conclusions and further work*

- ❖ We have open a promising avenue of research.
- ❖ We have found that the LICA can discover activations in agreement with the SPM in terms of activation detection in fMRI.
- ❖ Further work will be addressed to explore application of LICA:
  - In other fMRI experimental settings.
  - In other processing like VBM.





# *Contents*

- ❖ Introduction and Motivation
- ❖ MRI intensity inhomogeneity correction
- ❖ On the detection of Alzheimer's disease
- ❖ Lattice Computing for fMRI analysis
- ❖ Summary of conclusions



## *Summary of conclusions*

- ❖ The presentation of my dissertation has followed the historical evolution of my works on MRI:
  - Works on IIH correction:
    - GradClassLeg following the trend of a previous PhD in the research group.
    - AFR as a self organizing map inspired IIH field estimation.
  - Works on the diagnostic support of Alzheimer's disease.
  - A new research line on the application of Lattice Computing for fMRI.





## *Summary of conclusions*

- ❖ Regarding IIR correction algorithms and robust segmentation:
  - Our proposals have been formally well grounded on a widely accepted image formation model.
  - We have discussed and proved some convergence properties that ensure the theoretical performance of the algorithms.
  - We have realized extensive computational experiments showing:
    - that our algorithms are comparable or improve the state of the art algorithms.
    - the robustness of the algorithms against initial conditions.



## *Summary of conclusions*

- ❖ Regarding Alzheimer's disease diagnostic support:
  - We have proposed a feature extraction process from the MRI data based on VBM.
  - We have tested a number of classification approaches over a carefully selected subset of the OASIS database.
    - Results are reproducible.
    - Results are close to optimal results reported for other databases on similar problems.





## *Summary of conclusions*

- ❖ Regarding the application of Lattice Computing to fMRI:
  - We propose a Lattice Independent Component Analysis to the activity detection on fMRI data.
    - it is an unsupervised approach that can be applied with exploratory purposes.
  - We find agreement between at least one of the found endmembers' abundance and the supervised results of the SPM on this data.
    - this agreement is a kind of qualitative validation of the approach, opening the road for further experimentation.



*Thank you for your attention!*